Int. J. Radiation Oncology Biol. Phys., Vol. 79, No. 1, pp. 279–288, 2011

0360-3016/$–see front matter

ELSEVIER

doi:10.1016/j.ijrobp.2010.02.008

PHYSICS CONTRIBUTION

IMPACT OF FOUR-DIMENSIONAL COMPUTED TOMOGRAPHY PULMONARY VENTILATION IMAGING-BASED FUNCTIONAL AVOIDANCE FOR LUNG CANCER RADIOTHERAPY

TOKIHIRO YAMAMOTO, PH.D.,* SVEN KABUS, PH.D.,† JENS VON BERG, PH.D.,† CRISTIAN LORENZ, PH.D.,† AND PAUL J. KEALL, PH.D.*

*Department of Radiation Oncology, Stanford University School of Medicine, Stanford, CA; †Department of Digital Imaging, Philips Research Europe, Hamburg, Germany

Purpose: To quantify the dosimetric impact of four-dimensional computed tomography (4D-CT) pulmonary ventilation imaging-based functional treatment planning that avoids high-functional lung regions.
Methods and Materials: 4D-CT ventilation images were created from 15 non–small-cell lung cancer patients using deformable image registration and quantitative analysis of the resultant displacement vector field. For each patient, anatomic and functional plans were created for intensity-modulated radiotherapy (IMRT) and volumetric modulated arc therapy (VMAT). Consistent beam angles and dose–volume constraints were used for all cases. The plans with Radiation Therapy Oncology Group (RTOG) 0617–defined major deviations were modified until clinically acceptable. Functional planning spared the high-functional lung, and anatomic planning treated the lungs as uniformly functional. We quantified the impact of functional planning compared with anatomic planning using the two- or one-tailed *t* test.
Results: Functional planning led to significant reductions in the high-functional lung dose, without significantly increasing other critical organ doses, but at the expense of significantly degraded the planning target volume (PTV) conformity and homogeneity. The average reduction in the high-functional lung mean dose was 1.8 Gy for IMRT ($p < .001$) and 2.0 Gy for VMAT ($p < .001$). Significantly larger changes occurred in the metrics for patients with a larger amount of high-functional lung adjacent to the PTV.
Conclusion: The results of the present study have demonstrated the impact of 4D-CT ventilation imaging-based functional planning for IMRT and VMAT for the first time. Our findings indicate the potential of functional planning in lung functional avoidance for both IMRT and VMAT, particularly for patients who have high-functional lung adjacent to the PTV. © 2011 Elsevier Inc.

Lung cancer, functional imaging, four-dimensional computed tomography, 4D-CT, intensity-modulated radiotherapy, IMRT, volumetric modulated arc therapy, VMAT.

INTRODUCTION

Dose escalation is necessary to improve survival of lung cancer patients undergoing radiotherapy (1). However, dose escalation has been hampered by dose-limiting toxicity (*e.g.,* radiation pneumonitis and pulmonary fibrosis) that is potentially fatal. The incidence of pneumonitis has ranged from 2% to 31% for three-dimensional (3D) conformal radiotherapy (CRT) (2). It is clear that pulmonary toxicity increases with the lung dose (3). Although advanced techniques have enabled dose escalation simultaneously with sparing critical organs (1), the morbidity is still considerable (4). Yom *et al*. (4) demonstrated a significantly lower rate of Grade 3 or greater pneumonitis after intensity-modulated radiotherapy (IMRT) for advanced non–small-cell lung cancer (NSCLC) patients compared with 3D-CRT.

Radiotherapy that avoids high-functional lung regions might allow pulmonary toxicity reduction. This has been supported by the following findings. First, several studies have demonstrated that patients with lower pretreatment pulmonary function are more likely to develop toxicity than those with greater function (5, 6). Robnett *et al*. (6) found that no lung cancer patient developing severe pneumonitis had a pretreatment forced expiratory volume in 1 s(FEV_1) of >2.0 L, which might have been because a lower proportion of high-functional lung was damaged by radiation for such patients than those with

Reprint requests to: Tokihiro Yamamoto, Ph.D., Department of Radiation Oncology, Stanford University School of Medicine, 875 Blake Wilbur Dr., Stanford, CA 94305-5847. Tel: (650) 498-7104; Fax: (650) 498-5008; E-mail: Tokihiro@stanford.edu

Conflict of interest: S. Kabus, J. von Berg, and C. Lorenz are employees of Philips Research Europe.

Acknowledgments—Drs. Byungchul Cho and Yelin Suh at Stanford University provided technical assistance with the Pinnacle^3 treatment planning system.

Received Oct 7, 2009, and in revised form Jan 13, 2010. Accepted for publication Feb 8, 2010.

lower FEV_1. Second, several studies have indicated that the high-functional lung dose is a better predictor of toxicity (5, 7). Yorke *et al.* (7) demonstrated that the mean dose to the lower parts of the lung was more predictive of toxicity than that to the upper parts. The lower parts are known to have greater ventilation and greater blood flow than the upper parts (8). Therefore, lung functional avoidance has the potential to reduce pulmonary toxicity.

Regional functional information of the lung can be represented by ventilation (the subject of the present study) or perfusion. Several techniques have been used for regional ventilation imaging, including nuclear medicine imaging (9), hyperpolarized gas magnetic resonance imaging (10), and computed tomography (CT) imaging using xenon gas (11). However, these techniques have limitations, including a long scan time, low resolution, high cost, and/or low accessibility. A ventilation image is created by a novel four-dimensional (4D) CT-based technique in two steps, first by spatial regional mapping of different respiratory phases of 4D-CT images using deformable image registration (DIR), and second by quantitative analysis of the resultant displacement vector field (12–16). The 4D-CT–derived ventilation can be considered "free" information for lung cancer radiotherapy patients, because, in many centers, 4D-CT scans are routinely acquired during treatment planning, and ventilation computation involves only image processing. Moreover, 4D-CT–based ventilation imaging is faster, has higher resolution, and is more widely accessible than existing techniques.

The purpose of the present study was to quantify the impact of 4D-CT ventilation imaging-based functional planning compared with anatomic planning. Functional planning spared the high-functional lung, and anatomic planning treated the lungs as uniformly functional. We investigated two treatment scenarios: fixed-beam IMRT and volumetric modulated arc therapy (VMAT). VMAT is an emerging technique for delivering treatment efficiently in a single gantry rotation with continuous changes in the gantry speed, multileaf collimator (MLC) leaf position, and dose rate during irradiation. Recent studies have demonstrated highly conformal VMAT plans with significant reductions in the delivery time compared with IMRT and 3D-CRT for several sites (17, 18).

METHODS AND MATERIALS

Patients

The present study was a retrospective analysis approved by Stanford University's Institutional Review Board. We studied 15 patients, who had NSCLC and had undergone 4D-CT scanning and radiotherapy. The patient characteristics are listed in Table 1. More than one-half of the patients (60%) had Stage I NSCLC, and 5 of the 15 patients had more than one tumor. Treatment plans were created for a total of 21 tumors. The tumors were distributed relatively uniformly within the lungs.

Table 1. Patient characteristics

Parameter	Value
Age (y)	75.1 ± 9.0
Gender	
Male	10/15 (66.7)
Female	5/15 (33.3)
Histologic type	
NSCLC, adenocarcinoma	12/15 (80.0)
NSCLC, squamous cell carcinoma	1/15 (6.7)
NSCLC, NOS	2/15 (13.3)
Stage	
I	9/15 (60.0)
II	2/15 (13.3)
III	3/15 (20.0)
Metastatic tumor	1/15 (6.7)
Tumor number	
1	10/15 (66.7)
2	4/15 (26.7)
3	1/15 (6.7)
Tumor location	
Right upper left	4/21 (19.0)
Right lower left	6/21 (28.6)
Left upper left	7/21 (33.3)
Left lower left	4/21 (19.5)
PTV (cm^3)	234 ± 180
Total lung volume (cm^3)	3,945 ± 1,208

Abbreviations: NSCLC = non–small-cell lung cancer; NOS = not otherwise specified; PTV = planning target volume.

Data presented as mean ± standard deviation or numbers, with percentages in parentheses.

4D-CT–based ventilation imaging

Four-dimensional CT-based ventilation imaging consists of three steps. The first step was to acquire 4D-CT images for treatment planning purposes. We acquired 4D-CT scans using the GE Discovery ST multislice positron emission CT (PET)/CT scanner (GE Medical Systems, Waukesha, WI) in cine mode with the Varian Real-time Position Management (RPM) system (Varian Medical Systems, Palo Alto, CA). We investigated the exhale respiratory gating scenario, consistent with the current clinical practice at Stanford University for conventionally fractionated NSCLC patients. Paired 4D-CT images at the peak-exhale and peak-inhale phases were used for ventilation computation, and those at peak-exhale for treatment planning. Additional details on the 4D-CT acquisition have been previously published (19).

The second step was DIR for spatial voxel-wise mapping of the peak-exhale 4D-CT image to the peak-inhale image, deriving a displacement vector field. In the present study, we used nonparametric volume-based registration, the geometric accuracy of which has been previously validated (12). This registration algorithm is volumetric by itself and tries to find a vector field that minimizes both a similarity function and an elastic regularizer according to the Navier-Lamé equation.

The final step was the creation of a 4D-CT ventilation image through quantitative analysis of the displacement vector field. The Jacobian determinant of deformation (13) was used as a ventilation metric in the present study. The regional ventilation, $V(x,y,z)$, is given by

$$V(x,y,z) = \begin{vmatrix} 1+\frac{\partial u_x(x,y,z)}{\partial x} & \frac{\partial u_x(x,y,z)}{\partial y} & \frac{\partial u_x(x,y,z)}{\partial z} \\ \frac{\partial u_y(x,y,z)}{\partial x} & 1+\frac{\partial u_y(x,y,z)}{\partial y} & \frac{\partial u_y(x,y,z)}{\partial z} \\ \frac{\partial u_z(x,y,z)}{\partial x} & \frac{\partial u_y(x,y,z)}{\partial y} & 1+\frac{\partial u_z(x,y,z)}{\partial z} \end{vmatrix} - 1 \quad (1)$$

where $u(x, y, z)$ is the displacement vector mapping the voxel at location (x, y, z) of a peak-exhale image to the corresponding location of a peak-inhale image. Regional ventilation was determined for each voxel at the peak-exhale phase, resulting in a 4D-CT ventilation image.

Anatomic and functional treatment planning for IMRT or VMAT

Figure 1 shows a schematic diagram for creating an anatomic plan and 4D-CT ventilation imaging-based functional plan and quantifying the impact of functional planning compared with anatomic planning. In the present study, we investigated two treatment scenarios: fixed-beam IMRT and VMAT. Functional planning is based on the constraints on three functional lung regions (high-, moderate-, and low-functional lungs) determined as described in detail in the following sections. Anatomic planning is based on the constraints on the total lung. Contouring and treatment planning were performed using the Pinnacle[3] treatment planning system, version 8.9 (Philips Radiation Oncology Systems, Fitchburg, WI).

The gross tumor volume (GTV), clinical target volume (CTV), planning target volume (PTV), and critical organs, including the heart, spinal cord, esophagus, planning normal tissue volume (entire thorax minus the PTV), and lungs, were contoured on a peak-exhale 4D-CT image by one planner. The GTV to CTV and CTV to PTV margins were 5–8 mm and 8 mm, respectively. The spinal cord and esophagus were expanded by 5 mm to generate the planning organ-at-risk volumes (PRVs). In addition, three functional lung regions were defined from a 4D-CT ventilation image for functional planning by (*1*) zeroing the ventilation values outside the lungs, (*2*) computing a probability density function, (*3*) determining two threshold values that divided the total lung into three equal volumes, and (*4*) segmenting the functional lung regions. The three equal volumes have been termed high-, moderate-, and low-functional lungs throughout our report.

The beam arrangements for IMRT were six coplanar 6-MV photon beams fixed at gantry angles of 320°, 0°, 40°, 160°, 200°, and 240°. The VMAT plans consisted of a single coplanar arc 6-MV photon beam starting at a gantry angle of 0° and finishing at 356°, with continuous changes in the gantry speed, MLC leaf position, and dose rate. The collimator angle was fixed at 45° throughout the arc to minimize the MLC interleaf leakage and tongue-and-groove effects. The same beam arrangements were used for both anatomic and functional planning.

We prescribed 74 Gy in 37 fractions to 95% of the PTV. Table 2 lists the dose–volume constraints for each structure. The constraints on the total lung were used in anatomic planning, and those on the three functional lung regions were used in functional planning, with the greatest weight for the high-functional lung. We used an equivalent uniform dose (EUD) constraint, in addition to the dose–volume constraints, to reduce the mean dose to the high-functional lung. The tissue-specific parameter, α, was set to 2, according to Wu *et al*. (20). After convergence and converting to MLC segments, dose calculation was performed using the collapsed cone convolution implementation of the superposition algorithm. Segment weight optimization was then performed to recover potential convergence errors (21) introduced by the MLC delivery constraints not being included in optimization of the intensity distributions. To maintain both the scientific rigor and clinically acceptable plans, we used two planning strategies. First, we changed only one variable: the presence or absence of constraints on the functional lung (absence/presence plan), and, second, we modified the constraints and/or prescription dose as appropriate to conform to the Radiation Therapy Oncology Group (RTOG) 0617 protocol (clinically acceptable plan). For the absence/presence plans, we kept the constraints (Table 2) unchanged and prescribed 74 Gy to 95% of the PTV for

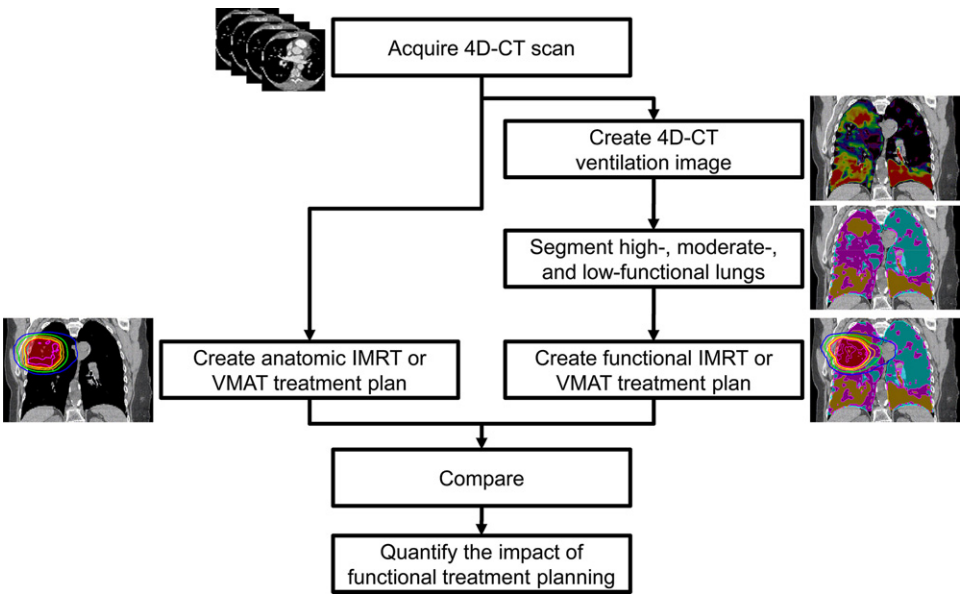

Fig. 1. Schematic diagram for creating anatomic treatment plan and four-dimensional (4D) computed tomography (CT) ventilation imaging-based functional plan and quantifying impact of functional planning. First step of functional planning was creation of 4D-CT ventilation image. Second step was segmentation of three functional lung regions with equal volumes: high-functional (orange), moderate-functional (pink), and low-functional (aqua) lung regions. Final step was creation of functional intensity-modulated radiotherapy (IMRT) or volumetric modulated arc therapy (VMAT) plan. Resultant functional plans were compared with anatomic plans to quantify impact of functional planning.

Table 2. Dose–volume constraints for anatomic and functional treatment planning used for intensity-modulated radiotherapy (IMRT) and volumetric modulated arc therapy (VMAT)

		Anatomic			Functional		
Structure	Constraint type	Dose (Gy)	Volume (%)	Weight	Dose (Gy)	Volume (%)	Weight
PTV	Minimum DVH	74.0	95	100	74.0	95	100
PTV	Minimum dose	66.6		40	66.6		40
PTV	Maximum dose	88.8		40	88.8		40
PTV	Minimum dose	74.0		10	74.0		10
PTV	Maximum dose	74.0		10	74.0		10
Heart	Maximum DVH	40.0	50	20	40.0	50	20
Heart	Maximum DVH	40.0	25	1	40.0	25	1
Spinal cord PRV	Maximum dose	45.0		50	45.0		50
Esophagus PRV	Maximum DVH	55.0	30	40	55.0	30	40
Esophagus PRV	Maximum DVH	40.0	30	1	40.0	30	1
Entire thorax minus PTV	Maximum dose	80.0		100	80.0		100
Total lung minus GTV	Maximum DVH	20.0	30	20			
Total lung minus GTV	Maximum DVH	20.0	15	1			
High-functional lung minus GTV	Maximum DVH				20.0	30	20
High-functional lung minus GTV	Maximum DVH				20.0	10	5
High-functional lung minus GTV	Maximum EUD*				21.0		20
Moderate-functional lung minus GTV	Maximum DVH				20.0	30	5
Low-functional lung minus GTV	Maximum DVH				20.0	30	0.2

Abbreviations: PTV = planning target volume; DVH = dose–volume histogram; PRV = planning organ-at-risk volume; GTV = gross tumor volume; EUD = equivalent uniform dose.

* Tissue-specific parameter, α, set to 2 for EUD calculation.

all plans to attain high consistency and comparability. For the clinically acceptable plans, we followed the process shown in Fig. 2:

1. Created plans using the baseline dose–volume constraints (Table 2) and prescribed 74 Gy to 95% of the PTV.
2. If the PTV dose was defined by the RTOG 0617 as a major deviation and/or the spinal cord dose did not meet the RTOG 0617 constraint, we increased the penalty of constraints on the PTV and/or spinal cord PRV.
3. If the PTV dose was still defined by the RTOG 0617 as a major deviation and/or the spinal cord dose did not meet the constraint, we modified the dose prescription such that 93% of the prescribed dose was between 99% and 95% of the PTV (minor deviation).

The RTOG 0617-defined major deviation of the PTV dose is that 93% of the prescribed dose is <95% of the PTV or a contiguous volume of $\leq$2 cm^3 inside the PTV is >125% of the prescribed dose. The minor deviation of dose prescription is that 93% of the prescribed dose is between 99% and 95% of the PTV or a contiguous volume of $\leq$2 cm^3 inside the PTV is between 120% and 125% of the prescribed dose. The spinal cord dose constraint was 50.5 Gy.

Statistical analysis

Statistical analyses were performed to quantify the impact of functional planning for both IMRT and VMAT. We tested whether the evaluation metrics of the functional plans were significantly different from those of anatomic plans ($p < .05$) using the two-tailed t test for all structures, except for functional lungs, for which we tested whether the functional lung doses of the functional plans were significantly lower than those of the anatomic plans using the one-tailed t test. Given that the impact of functional planning is expected to be large for patients who have a large amount of high-functional lung adjacent to the PTV, we compared the changes in evaluation metrics for a subgroup of patients (n = 8) with greater overlap between the high-functional lung and the PTV with those for a subgroup (n = 7) with less overlap, using the Wilcoxon rank-sum test.

RESULTS

Comparison between anatomic and functional treatment plans for example patient

Figure 3 shows the isodose distributions and dose–volume histograms (DVHs) of the clinically acceptable anatomic and functional plans for IMRT (Fig. 3a) and VMAT (Fig. 3b) for one patient. From a visual inspection of the isodose distributions, both functional IMRT and VMAT planning spared the high-functional lungs compared with anatomic planning. In particular, the 20- and 40-Gy isodose curves were significantly distorted and moved toward the left lung, which had less high-functional lung. Functional VMAT planning more clearly demonstrated the distortions of such isodose curves owing to its inherent nature of beam angle optimization. Functional IMRT planning showed considerable distortions of the isodose curves ($\geq$70 Gy) around the PTV compared with anatomic IMRT. Functional planning resulted in DVH curves clearly separated from those of anatomic planning (*e.g.,* lower high-functional lung dose, degraded PTV homogeneity, and increased esophagus PRV dose). For example, the homogeneity index of 1.07 in the anatomic IMRT plan increased to 1.19 with functional planning and from 1.15 to 1.16 for

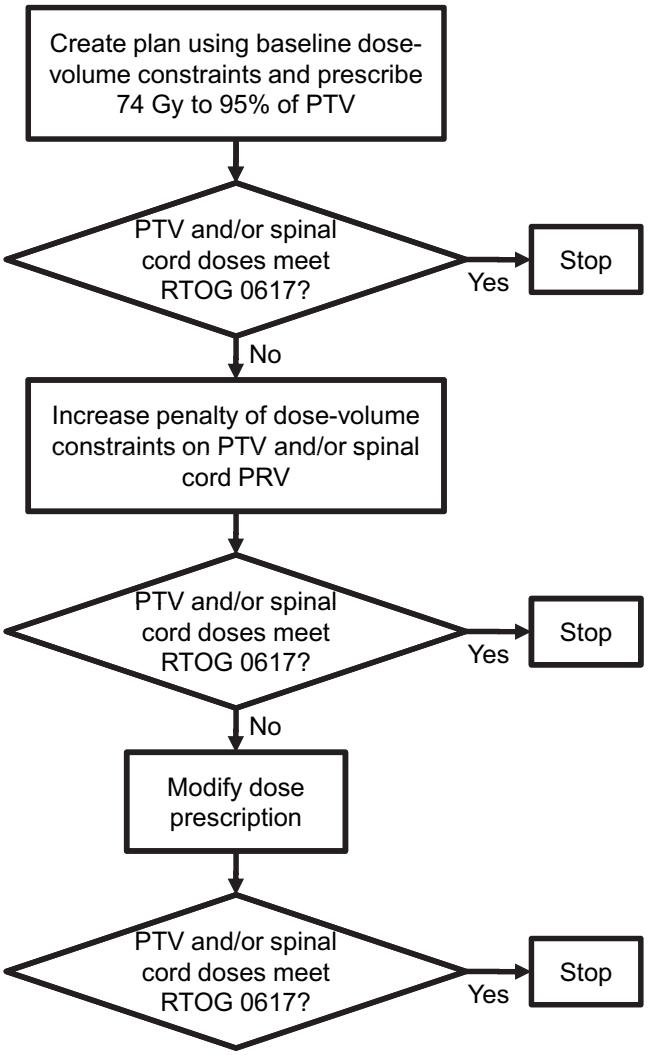

Fig. 2. Schematic diagram for creating clinically acceptable treatment plan through modification of constraints and/or prescription, as appropriate, to conform to Radiation Therapy Oncology Group (RTOG) 0617 protocol. PTV = planning target volume; PRV = planning organ-at-risk volume.

VMAT. The moderate-functional lung dose was similar for both plans; thus, those DVH curves were not shown in Fig. 3. In addition, functional planning resulted in increases in the esophagus PRV mean dose by 5.0 Gy for IMRT and 4.7 Gy for VMAT and decreases in the spinal cord PRV maximum dose by 3.7 Gy for IMRT and 6.8 Gy for VMAT.

Impact of functional IMRT and VMAT planning

For clinically acceptable planning, increasing the penalty of the constraints on the PTV and/or spinal cord PRV was necessary in 0 of the 15 patients for anatomic IMRT, 7 of 15 patients for functional IMRT, 1 of 15 patients for anatomic VMAT, and 4 of 15 patients for functional VMAT. Modifying the dose prescription was necessary in 0 of 15 patients for anatomic IMRT, 3 of 15 patients for functional IMRT, 0 of 15 patients for anatomic VMAT, and 4 of 15 patients for functional VMAT. Figure 4 shows comparisons of the evaluation metrics for the three functional lung regions between the anatomic and functional plans. For both IMRT and VMAT, functional planning led to a significantly lower high-functional lung dose compared with anatomic planning in the absence/presence plans. The reductions in the clinically acceptable plans were comparable to, or more significant than, those in the absence/presence plans. For the absence/presence plans, the high-functional lung mean dose of 14.7 $\pm$ 11.3 Gy in the anatomic IMRT plans was reduced to 13.0 $\pm$ 9.8 Gy ($p < .001$) by functional planning and from 16.9 $\pm$ 10.7 Gy to 15.3 $\pm$ 10.4 Gy ($p = .007$) for VMAT (Fig. 4a). For the clinically acceptable plans, the high-functional lung mean dose of 13.4 $\pm$ 8.2 Gy in the anatomic IMRT plans was reduced to 11.6 $\pm$ 6.9 Gy ($p < 0.001$) by functional planning and from 15.9 $\pm$ 8.8 Gy to 13.9 $\pm$ 7.7 Gy ($p < .001$) for VMAT (Fig. 4c). Nonsignificant differences were found in the moderate- and low-functional lung doses, except for the moderate-functional lung dose in the clinically acceptable IMRT plans.

Table 3 lists the comparisons of the metrics for the total lung, heart, spinal cord PRV, and esophagus PRV between the anatomic and functional plans. Functional planning resulted in total lung doses comparable to those with anatomic planning in the absence/presence plans and lower doses in the clinically acceptable plans. For other critical organs, functional planning led to greater doses than anatomic planning; however, the increases in the evaluation metrics were not significant. The increases in the clinically acceptable plans were consistently smaller than those in the absence/presence plans, and the p-values were consistently greater.

Table 4 lists the comparisons of the PTV metrics between the anatomic and functional plans. For both IMRT and VMAT, functional planning led to significantly degraded PTV conformity and homogeneity compared with anatomic planning in both the absence/presence and the clinically acceptable plans. For the absence/presence plans, the homogeneity index of 1.15 $\pm$ 0.18 in the anatomic IMRT plans was increased to 1.31 $\pm$ 0.43 ($p = 0.028$) by functional planning and from 1.10 $\pm$ 0.06 to 1.21 $\pm$ 0.17 ($p = .003$) for VMAT. For the clinically acceptable plans, the homogeneity index of 1.10 $\pm$ 0.06 in the anatomic IMRT plans was increased to 1.17 $\pm$ 0.10 ($p = .001$) by functional planning and from 1.09 $\pm$ 0.05 to 1.16 $\pm$ 0.10 ($p = .002$) for VMAT. Functional planning also resulted in significantly greater monitor units than in anatomic planning, as expected with the increased constraints for functional planning. Moreover, all PTV metrics of the functional plans, except for the conformity index in the absence/presence IMRT plans, resulted in larger standard deviations than those of the anatomic plans, indicating the varying impact of functional planning.

Changes in the high-functional lung, spinal cord PRV, and PTV metrics with functional planning are summarized for two subgroups of patients with greater overlap (high-overlap; 8 of 15 patients) and less overlap (low-overlap; 7 of 15

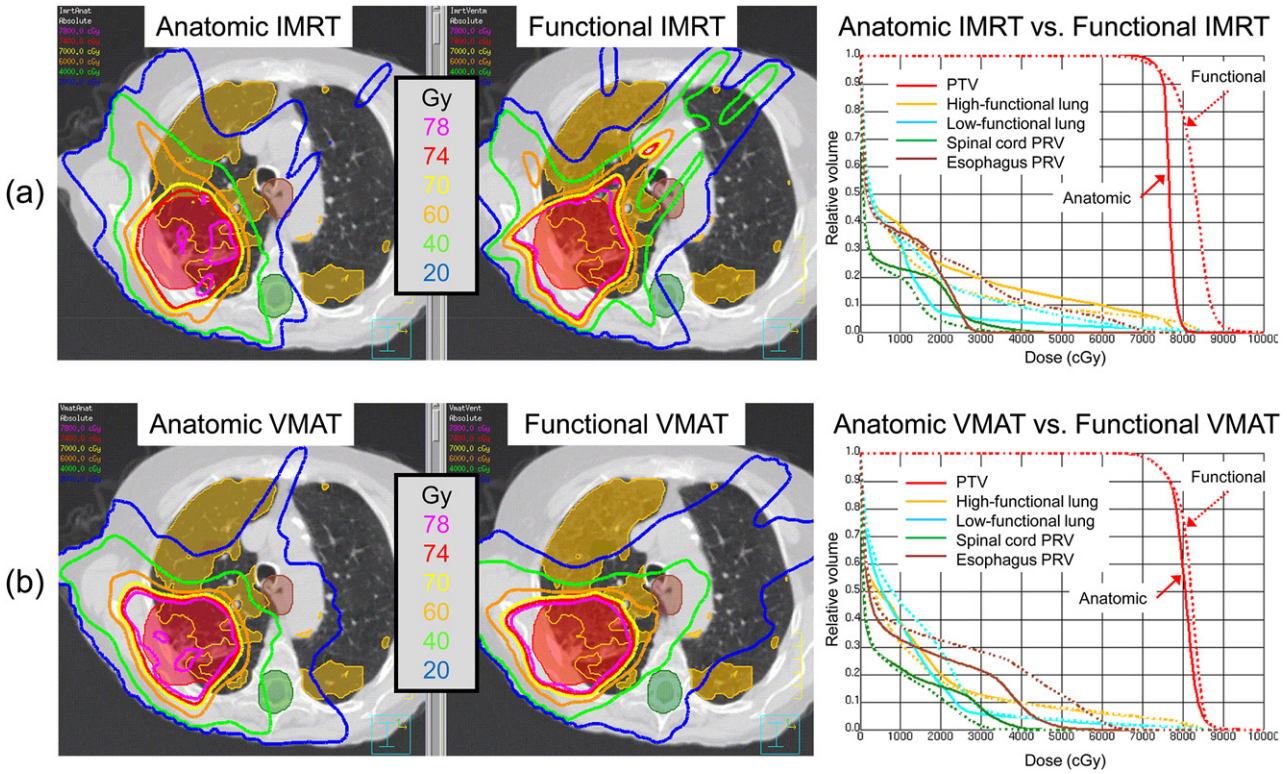

Fig. 3. Example isodose distributions and dose–volume histograms (DVHs) of (a) clinically acceptable anatomic and functional intensity-modulated radiotherapy (IMRT) plans, and (b) clinically acceptable anatomic and functional volumetric modulated arc therapy (VMAT) plans. In isodose distributions, high-functional lung region shaded orange; PTV, red; spinal cord planning organ-at-risk volume (PRV), green; and esophagus PRV, brown. In DVHs, anatomic plans represented by solid curves, and functional plans by dashed lines.

patients) between the high-functional lung and PTV in Table 5. Large differences were seen in the changes between the high-overlap subgroup and the low-overlap subgroup, especially in the absence/presence plans, and more than one-half of the metrics indicated significant changes. The high-overlap subgroup showed larger changes (*e.g.,* larger reductions in the high-functional lung dose with functional planning), and the low-overlap subgroup showed very small changes, with median values close to 0. These results have demonstrated that functional planning would have a high impact for patients who have a large amount of high-functional lung adjacent to the PTV.

DISCUSSION

We have demonstrated that 4D-CT ventilation imaging-based functional IMRT and VMAT treatment planning, by changing only one variable (*i.e.,* absence/presence plan), led to significant reductions in the high-functional lung dose without significantly increasing the doses to the other critical organs compared with anatomic planning, at the expense of significantly degraded PTV conformity and homogeneity. Modifying the constraints and/or prescription (*i.e.,* clinically acceptable plan) resulted in comparable or greater significant reductions in the high-functional lung dose and less significant increases in the other critical organ doses. Degradations in the PTV conformity and homogeneity were still significant in the clinically acceptable plans. Several studies have compared functional planning and anatomic planning for lung cancer (22–26). These studies were considerably different from each other in their optimization approach, definition of functional lung regions, treatment technique, and functional imaging technique. Although a detailed comparison would be difficult because of such diversities, all these studies demonstrated clear reductions in the high-functional lung dose with functional planning, at least for a particular group of patients, consistent with our findings. However, an inconsistency was found in the results of the PTV metrics. Shioyama *et al.* (22) showed significantly degraded conformity and a lower minimum dose as a tradeoff, consistent with the present study. In contrast, others (24, 25), showed comparable homogeneity. Yaremko *et al.* (23) demonstrated both degraded and comparable homogeneities using two different sets of constraints, both of which gave reductions in the high-functional lung dose. This inconsistency could be attributed mainly to the difference in the optimization approach, especially for the PTV metrics. Our findings have indicated the need for an optimization approach with an increased weight on the PTV homogeneity in functional planning, which was also discussed by Yaremko *et al.* (23).

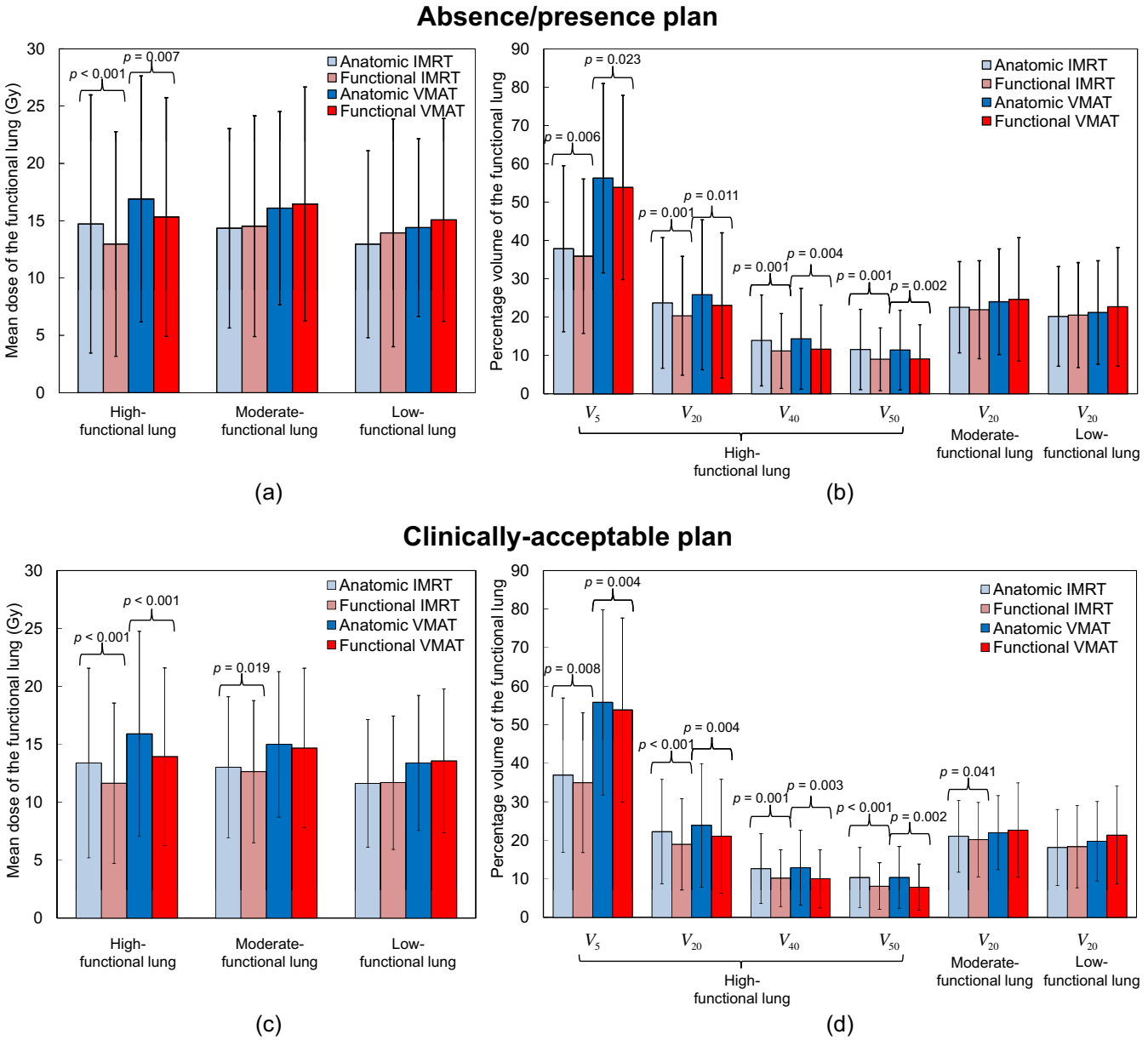

Fig. 4. Comparisons of (a) mean dose (mean ± standard deviation) and (b) percentage of volume receiving ≥5, ≥20, ≥40, or ≥50 Gy (V_5, V_{20}, V_{40}, V_{50}, respectively) for the three functional lung regions between absence/presence anatomic and functional treatment plans, and (c,d) those between clinically acceptable anatomic and functional plans for 15 lung cancer patients. The *p*-values shown only for statistically significant differences between metrics of anatomic and functional plans.

Fixed-beam IMRT and VMAT were investigated for the first time in the present study, and functional IMRT and VMAT planning were found to have a similar impact to each other on the high-functional lung dose, PTV metrics, and doses to other critical organs. VMAT has an inherent nature of beam angle optimization, in addition to intensity map optimization, and IMRT is capable of intensity map optimization only. Such an additional degree of freedom in optimization might lead to a superior functional VMAT plan compared with a functional IMRT plan. Lavrenkov *et al.* (27) compared functional IMRT planning and functional 3D-CRT planning using single photon emission CT (SPECT) perfusion images and demonstrated that functional IMRT planning led to a significantly lower high-functional lung mean dose than did functional 3D-CRT planning.

We have clearly demonstrated that the impact of functional treatment planning is significant for patients with greater overlap between the high-functional lung and the PTV. The impact of functional planning was very small for patients with less overlap, because anatomic planning for such patients would deposit relatively lower doses to

Table 3. Critical organ metrics of anatomic and functional treatment plans for 15 lung cancer patients

Metric	Planning strategy	IMRT			VMAT		
		Anatomic	Functional	*p*	Anatomic	Functional	*p*
Total lung; mean dose (Gy)							
	Absence/presence	12.9 ± 5.6	12.8 ± 6.3	.690	15.1 ± 6.3	15.1 ± 7.6	.960
	Clinically acceptable	12.7 ± 5.3	12.0 ± 5.1	.006	14.8 ± 5.9	14.1 ± 6.1	.056
Heart; V_{40} (Gy)							
	Absence/presence	8.3 ± 15.3	10.9 ± 18.6	.079	5.5 ± 11.5	9.2 ± 17.8	.053
	Clinically acceptable	8.1 ± 15.0	9.5 ± 16.4	.235	5.4 ± 11.6	7.4 ± 15.4	.145
Spinal cord PRV; maximum dose (Gy)							
	Absence/presence	40.2 ± 22.0	45.4 ± 27.1	.030	43.1 ± 17.0	47.3 ± 21.0	.067
	Clinically acceptable	40.0 ± 21.9	40.8 ± 23.0	.433	42.9 ± 16.9	43.7 ± 17.5	.449
Esophagus PRV; mean dose (Gy)							
	Absence/presence	11.4 ± 8.2	12.4 ± 9.2	.104	15.3 ± 9.5	16.2 ± 10.3	.373
	Clinically acceptable	11.1 ± 8.0	11.6 ± 8.6	.358	15.1 ± 9.2	15.3 ± 9.3	.807

Abbreviations: IMRT = intensity-modulated radiotherapy; VMAT = volumetric modulated arc therapy; V_x = percentage of volume receiving ≥x Gy; PRV = planning organ-at-risk volume.

Data presented as mean ± standard deviation.

the high-functional lung regions. However, an extremely high overlap would pose a challenging optimization problem and could lead to a substantial tradeoff between the high-functional lung dose and PTV homogeneity. A pattern of the functional lung distribution depends on how to define the functional lung regions, which has varied considerably from investigator to investigator (22–25). Additional studies are needed to investigate how to optimally define the functional lung.

Four-dimensional CT-based ventilation imaging is faster, has higher resolution, is more widely accessible, and is more cost effective than existing techniques. However, variations in the DIR results between algorithms have been reported (28). We also found that different DIR algorithms and different metrics yielded variant ventilation images (unpublished data). Although several investigators have validated the 4D-CT–based ventilation imaging technique to some extent (13, 15, 16), the regional physiologic accuracy has not been validated in patients. Also, temporal changes might occur in the regional ventilation during the radiotherapy course. For example, shrinkage of the lung tumor volume in response to treatment would result in an increase in ventilation owing to reopening of the airways (29). Given these limitations, the present study, quantifying the impact of functional planning, should be seen as presenting an upper limit of the expected dosimetric benefit. Additional study validating the physiologic accuracy of 4D-CT–based ventilation imaging in patients and quantifying the impact of temporal changes in ventilation during the treatment course are needed.

Table 4. Planning target volume (PTV) metrics of anatomic and functional treatment plans for 15 lung cancer patients

Metric	Planning strategy	IMRT			VMAT		
		Anatomic	Functional	*p*	Anatomic	Functional	*p*
Mean dose (Gy)							
	Absence/presence	79.9 ± 6.6	85.3 ± 11.2	.004	78.3 ± 2.8	83.5 ± 8.3	.003
	Clinically acceptable	77.9 ± 2.6	80.1 ± 3.3	.018	78.0 ± 2.4	79.8 ± 3.2	.013
Conformity index*							
	Absence/presence	0.57 ± 0.18	0.51 ± 0.17	.004	0.66 ± 0.16	0.60 ± 0.18	.009
	Clinically acceptable	0.63 ± 0.08	0.58 ± 0.09	.010	0.70 ± 0.05	0.67 ± 0.08	.047
Homogeneity index†							
	Absence/presence	1.15 ± 0.18	1.31 ± 0.43	.028	1.10 ± 0.06	1.21 ± 0.17	.003
	Clinically acceptable	1.10 ± 0.06	1.17 ± 0.10	.001	1.09 ± 0.05	1.16 ± 0.10	.002
Monitor units							
	Absence/presence	624 ± 252	921 ± 503	.002	355 ± 73	444 ± 128	<.001
	Clinically acceptable	602 ± 219	843 ± 373	.001	358 ± 77	420 ± 95	.011

Abbreviations: PTV = planning target volume; other abbreviations as in Table 3.

* Conformity index = cover factor × spill factor, where cover factor defined as relative PTV receiving ≥74 Gy, and spill factor defined as ratio of PTV receiving ≥74 Gy to total volume receiving 74 Gy.

† Homogeneity index = $D_{5\%}/D_{95\%}$, where $D_{x\%}$ is minimum dose in x% of PTV.

Table 5. Changes in high-functional lung, spinal cord planning organ-at-risk volume (PRV), and planning target volume (PTV) metrics with functional treatment planning compared with anatomic planning for high-overlap and low-overlap subgroups

		IMRT			VMAT		
Metric	Planning strategy	High-overlap (n = 8)	Low-overlap (n = 7)	p	High-overlap (n = 8)	Low-overlap (n = 7)	p
High-functional lung							
Mean dose (Gy)							
	Absence/presence	−3.1 (−5.5, −1.4)	0.0 (-2.0, 0.2)	.001	−2.1 (−6.2, 1.3)	−0.1 (−2.9, 0.3)	.094
	Clinically acceptable	−3.1 (−4.2, −1.8)	0.0 (−2.0, 0.2)	.001	−3.4 (−5.3, −1.0)	−0.1 (−2.9, 0.3)	.004
V_{20} (%)							
	Absence/presence	−5.1 (−10.1, −0.3)	−0.3 (−3.2, 0.1)	.002	−2.2 (−12.0, 1.0)	0.0 (−7.5, 1.2)	.072
	Clinically acceptable	−5.5 (−10.2, −1.7)	−0.3 (−3.2, 0.1)	.001	−4.3 (−9.6, 1.2)	0.0 (−7.5, 1.2)	.054
V_{40} (%)							
	Absence/presence	−4.6 (−7.7, −2.0)	0.0 (−4.9, 0.7)	.006	−4.0 (−11.0, −0.1)	0.0 (−5.0, 0.7)	.014
	Clinically acceptable	−4.6 (−7.7, −2.0)	0.0 (−4.9, 0.7)	.009	−3.7 (−11.0, −0.1)	0.0 (−5.0, 0.7)	.026
Spinal cord PRV							
Maximum dose (Gy)	Absence/presence	11.6 (−6.1, 21.9)	0.0 (−2.6, 2.2)	.014	6.8 (−6.8, 20.1)	0.2 (−4.4, 9.1)	.152
	Clinically acceptable	2.0 (−5.6, 10.3)	0.0 (−2.6, 2.2)	.189	1.6 (−6.8, 5.9)	0.2 (−4.4, 9.1)	.397
PTV							
Mean dose (Gy)							
	Absence/presence	8.7 (−1.7, 17.6)	0.1 (−0.8, 6.3)	.012	8.0 (1.1, 19.1)	0.3 (−0.6, 3.8)	<.001
	Clinically acceptable	1.8 (−1.3, 8.7)	0.1 (−0.8, 6.3)	.189	1.7 (0.0, 7.6)	0.2 (−0.6, 3.8)	.072
Conformity index							
	Absence/presence	−0.12 (−0.20, 0.02)	−0.01 (−0.06, 0.02)	.091	−0.10 (−0.23, 0.01)	0.01 (−0.17, 0.03)	.055
	Clinically acceptable	−0.10 (−0.19, 0.02)	−0.01 (−0.06, 0.02)	.152	−0.05 (−0.10, 0.01)	0.01 (−0.17, 0.03)	.121
Homogeneity index							
	Absence/presence	0.19 (0.03, 1.09)	0.00 (−0.03, 0.13)	.001	0.17 (0.01, 0.37)	0.00 (−0.01, 0.07)	.001
	Clinically acceptable	0.13 (0.04, 0.18)	0.00 (−0.03, 0.13)	.009	0.13 (0.01, 0.16)	0.00 (−0.01, 0.07)	.002
Monitor units							
	Absence/presence	508 (106, 903)	2 (−145, 308)	.002	177 (−94, 279)	0 (−14, 85)	.016
	Clinically acceptable	419 (165, 624)	2 (−145, 308)	.001	138 (−94, 177)	0 (−14, 85)	.029

Abbreviations as in Tables 2 and 3.
Data presented as median, with minimum and maximum in parentheses.

CONCLUSION

The present study has demonstrated the dosimetric impact of 4D-CT ventilation imaging-based functional treatment planning for IMRT and VMAT for the first time. For both IMRT and VMAT, functional planning led to significant reductions in the high-functional lung dose, without significantly increasing the dose to the other critical organs compared with anatomic planning. However, the PTV conformity and homogeneity were significantly degraded. Our findings have indicated the potential of 4D-CT ventilation imaging-based functional planning in lung functional avoidance for both IMRT and VMAT, particularly for patients with high-functional lung adjacent to the PTV.

REFERENCES

1. Onishi H, Araki T, Shirato H, *et al*. Stereotactic hypofractionated high-dose irradiation for stage I nonsmall cell lung carcinoma: Clinical outcomes in 245 subjects in a Japanese multiinstitutional study. *Cancer* 2004;101:1623–1631.
2. Kong FM, Ten Haken R, Eisbruch A, *et al*. Non-small cell lung cancer therapy-related pulmonary toxicity: An update on radiation pneumonitis and fibrosis. *Semin Oncol* 2005;32:S42–S54.
3. Kong FM, Hayman JA, Griffith KA, *et al*. Final toxicity results of a radiation-dose escalation study in patients with non–small-cell lung cancer (NSCLC): Predictors for radiation pneumonitis and fibrosis. *Int J Radiat Oncol Biol Phys* 2006;65:1075–1086.
4. Yom SS, Liao Z, Liu HH, *et al*. Initial evaluation of treatment-related pneumonitis in advanced-stage non–small-cell lung cancer patients treated with concurrent chemotherapy and intensity-modulated radiotherapy. *Int J Radiat Oncol Biol Phys* 2007;68:94–102.
5. Lind PA, Marks LB, Hollis D, *et al*. Receiver operating characteristic curves to assess predictors of radiation-induced symptomatic lung injury. *Int J Radiat Oncol Biol Phys* 2002;54:340–347.
6. Robnett TJ, Machtay M, Vines EF, *et al*. Factors predicting severe radiation pneumonitis in patients receiving definitive chemoradiation for lung cancer. *Int J Radiat Oncol Biol Phys* 2000;48:89–94.
7. Yorke ED, Jackson A, Rosenzweig KE, *et al*. Dose–volume factors contributing to the incidence of radiation pneumonitis in non–small-cell lung cancer patients treated with three-dimensional conformal radiation therapy. *Int J Radiat Oncol Biol Phys* 2002;54:329–339.
8. Levitzky MG. Pulmonary physiology. 7th ed. New York: McGraw-Hill Medical; 2007.
9. Suga K. Technical and analytical advances in pulmonary ventilation SPECT with xenon-133 gas and Tc-99m-Technegas. *Ann Nucl Med* 2002;16:303–310.
10. Kauczor H, Surkau R, Roberts T. MRI using hyperpolarized noble gases. *Eur Radiol* 1998;8:820–827.

11. Simon BA. Regional ventilation and lung mechanics using X-Ray CT. *Acad Radiol* 2005;12:1414–1422.
12. Kabus S, von Berg J, Yamamoto T, *et al*. Lung ventilation estimation based on 4D-CT imaging. Proceedings of the First International Workshop on Pulmonary Image Analysis, MICCAI 2008. 2008. pp. 73–81.
13. Reinhardt JM, Ding K, Cao K, *et al*. Registration-based estimates of local lung tissue expansion compared to xenon CT measures of specific ventilation. *Med Image Anal* 2008;12:752–763.
14. Christensen GE, Song JH, Lu W, *et al*. Tracking lung tissue motion and expansion/compression with inverse consistent image registration and spirometry. *Med Phys* 2007;34:2155–2163.
15. Guerrero T, Sanders K, Castillo E, *et al*. Dynamic ventilation imaging from four-dimensional computed tomography. *Phys Med Biol* 2006;51:777–791.
16. Guerrero T, Sanders K, Noyola-Martinez J, *et al*. Quantification of regional ventilation from treatment planning CT. *Int J Radiat Oncol Biol Phys* 2005;62:630–634.
17. Lagerwaard FJ, Meijer OW, van der Hoorn EA, *et al*. Volumetric modulated arc radiotherapy for vestibular schwannomas. *Int J Radiat Oncol Biol Phys* 2009;74:610–615.
18. Palma D, Vollans E, James K, *et al*. Volumetric modulated arc therapy for delivery of prostate radiotherapy: Comparison with intensity-modulated radiotherapy and three-dimensional conformal radiotherapy. *Int J Radiat Oncol Biol Phys* 2008;72:996–1001.
19. Yamamoto T, Langner U, Loo BW Jr., *et al*. Retrospective analysis of artifacts in four-dimensional CT images of 50 abdominal and thoracic radiotherapy patients. *Int J Radiat Oncol Biol Phys* 2008;72:1250–1258.
20. Wu Q, Djajaputra D, Liu HH, *et al*. Dose sculpting with generalized equivalent uniform dose. *Med Phys* 2005;32:1387–1396.
21. Siebers JV, Lauterbach M, Keall PJ, *et al*. Incorporating multileaf collimator leaf sequencing into iterative IMRT optimization. *Med Phys* 2002;29:952–959.
22. Shioyama Y, Jang SY, Liu HH, *et al*. Preserving functional lung using perfusion imaging and intensity-modulated radiation therapy for advanced-stage non-small cell lung cancer. *Int J Radiat Oncol Biol Phys* 2007;68:1349–1358.
23. Yaremko BP, Guerrero TM, Noyola-Martinez J, *et al*. Reduction of normal lung irradiation in locally advanced non–small-cell lung cancer patients, using ventilation images for functional avoidance. *Int J Radiat Oncol Biol Phys* 2007;68:562–571.
24. McGuire SM, Zhou S, Marks LB, *et al*. A methodology for using SPECT to reduce intensity-modulated radiation therapy (IMRT) dose to functioning lung. *Int J Radiat Oncol Biol Phys* 2006;66:1543–1552.
25. Christian JA, Partridge M, Nioutsikou E, *et al*. The incorporation of SPECT functional lung imaging into inverse radiotherapy planning for non-small cell lung cancer. *Radiother Oncol* 2005;77:271–277.
26. Seppenwoolde Y, Engelsman M, De Jaeger K, *et al*. Optimizing radiation treatment plans for lung cancer using lung perfusion information. *Radiother Oncol* 2002;63:165–177.
27. Lavrenkov K, Christian JA, Partridge M, *et al*. A potential to reduce pulmonary toxicity: The use of perfusion SPECT with IMRT for functional lung avoidance in radiotherapy of non-small cell lung cancer. *Radiother Oncol* 2007;83:156–162.
28. Kashani R, Hub M, Balter JM, *et al*. Objective assessment of deformable image registration in radiotherapy: A multi-institution study. *Med Phys* 2008;35:5944–5953.
29. Seppenwoolde Y, Muller SH, Theuws JC, *et al*. Radiation dose–effect relations and local recovery in perfusion for patients with non–small-cell lung cancer. *Int J Radiat Oncol Biol Phys* 2000;47:681–690.